Cell, Vol. 82, 193–207, July 28, 1995, Copyright © 1995 by Cell Press

Crystal Structure of the Site-Specific Recombinase γδ Resolvase Complexed with a 34 bp Cleavage Site

Wei Yang* and Thomas A. Steitz*†
*Department of Molecular Biophysics and Biochemistry
†Department of Chemistry
and Howard Hughes Medical Institute
Yale University
New Haven, Connecticut 06520

Summary

The structure of γδ resolvase complexed with a 34 bp substrate DNA has been determined at 3.0 Å resolution. The DNA is sharply bent by 60° toward the major groove and away from the resolvase catalytic domains at the recombination crossover point. The C-terminal one third of resolvase, which was disordered in the absence of DNA, forms an arm and a 3-helix DNA-binding domain on the opposite side of the DNA from the N-terminal domain. The arms wrap around the minor groove of the central 16 bp, and the DNA-binding domains interact with the major grooves near the outer boundaries of the binding site. The resolvase dimer is asymmetric, particularly in the arm region, implying a conformational adaptability that may be important for resolvase binding to different DNA sites in the synaptosome. It also raises the possibility of a sequential single-strand cleavage mechanism.

Introduction

γδ resolvase is a 183 amino acid site-specific recombinase encoded by transposon γδ, a natural component of the Escherichia coli F episome, and belongs to the resolvase and DNA invertase family (for reviews, see Hatfull and Grindley, 1988; Grindley, 1994). γδ resolvase forms a homodimer in solution and converts a negatively supercoiled circular DNA containing two directly repeated copies of a 114 bp recombination site, called *res*, into two catenated molecules via double-strand DNA cleavage, strand exchange, and religation (Figure 1a). When cleavage occurs, a phosphodiester bond is replaced by a phosphoserine bond between a 5′ phosphate group at the cleavage site and a hydroxyl group of Ser-10 in resolvase (Reed and Grindley, 1981; Reed and Moser, 1984). This site-specific recombination can take place in vitro and requires only resolvase, a substrate DNA, and multivalent cations (Reed, 1981). By the omission of multivalent cations, a cleaved DNA intermediate covalently linked to resolvase can be trapped; recombination resumes with the addition of multivalent cations. The 114 bp *res* sequence contains three resolvase-binding sites, I, II, and III (Figure 1b). Each binding site contains an inverted repeat of a 12 bp recognition sequence and binds a dimer of resolvase. The three sites differ, however, in the number and sequence of the base pairs between each inverted repeat. Double-strand cleavage and religation occur specifically at the center of site I (the crossover point), but the presence of sites II and III is essential for the cleavage to occur (Grindley et al., 1982; Bednarz et al., 1990). Two *res* DNAs combine with six resolvase dimers to form a compact, globular so-called synaptosome preceding the recombination reaction, as shown by electron microscopy (Benjamin and Cozzarelli, 1988).

Native γδ resolvase contains two additional activities. Topoisomerase I activity can be detected under optimal conditions for recombination (Krasnow and Cozzarelli, 1983) and is enhanced when recombination is impaired owing to mutations either around the active site of resolvase or at the crossover point in the DNA (Falvey et al., 1988; Leschziner et al., 1995). Resolvase also serves as its own transcriptional repressor, even when residues essential for catalysis are mutated (Newman and Grindley, 1984).

The crystal structure of an N-terminal chymotryptic fragment of γδ resolvase (residues 1–140) has been determined (Sanderson et al., 1990) and refined at 2.3 Å resolution (Rice and Steitz, 1994a). Only the first 120 residues of the fragment were ordered in this crystal as well as in the intact resolvase crystallized in a different lattice (Rice and Steitz, 1994b). These 120 residues form a conserved globular domain that contains the active site Ser-10, the dimer interface, and residues crucial for higher order interactions between resolvase dimers (Hughes et al., 1990, 1993). The C-terminal chymotryptic fragment (residues 141–183) contains sequence homologous to the helix-turn-helix (HTH) motif and binds specifically to the 12 bp consensus sequence in adjacent major and minor grooves, as shown by solution studies (Abdel-Meguid et al., 1984; Rimphanitchayakit et al., 1989).

We have determined the crystal structure of γδ resolvase dimer complexed with a 34 bp site I DNA analog at 3.0 Å resolution. This structure shows the following: first, the conformation of the last 63 residues that were disordered in the absence of DNA; second, the DNA kinked by 60° at its center and bent away from the catalytic domains; third, novel interactions between a pair of α helices and the DNA minor groove; and fourth, adaptability in both resolvase and site I DNA that provides the structural bases for the association of resolvase with sites II and III. This structure also raises the possibility of a sequential single-strand cleavage mechanism of the *res* DNA.

Results and Discussion

Structure of the Resolvase-DNA Complex

γδ resolvase was complexed and cocrystallized with a 34 bp DNA composed of two identical modules of the right half of site I annealed together through the central 8 bp (Figures 1b and 1c) (see Schultz et al., 1990). *res* DNA with a symmetrized site I consisting of two right halves of the natural sequence behaved similarly to the wild type in recombination (Bednarz et al., 1990). To achieve the

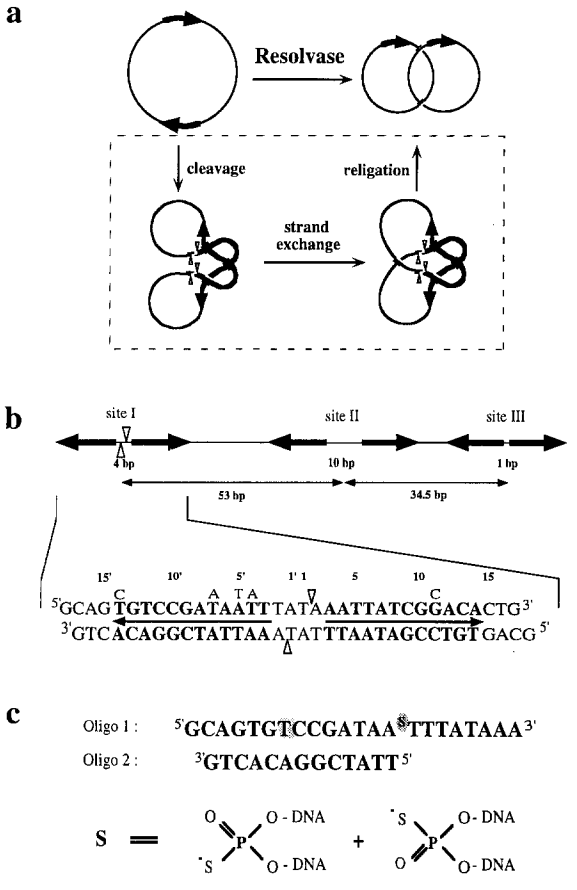

Figure 1. Recombination, *res*, and the DNA in the Crystal

(a) Resolvase resolves a negatively supercoiled DNA containing two directly repeated *res* sites, presented by the thick arrows, into two catenated DNA molecules. The three steps, DNA cleavage, strand exchange, and religation, are shown in the broken-line box. The positions of the DNA cleavages are indicated by the open triangles. Accompanying the recombination, three negative supercoils are trapped upon the formation of the synaptosome, and a right-handed strand exchange results in the singly catenated products.

(b) The 114 bp *res* DNA contains three binding sites for resolvase dimers, labeled I, II, and III. Each binding site has a pair of conserved 12 bp inverted repeats (represented by arrows). The sequence of the site I DNA analog cocrystallized with resolvase is shown, with the original sequence in italics above the mutated bases. The scissile bonds are again indicated by open triangles.

(c) The sequences of the two oligonucleotides used to generate a module of half a binding site are shown. The phosphate replaced by phosphorothioate is indicated by S in an oval (a racemic mixture of the diastereomers), and the thymidine substituted by iodouracil is stippled.

highest affinity for resolvase, the right half of site I with a G to C mutation was selected for the crystallization studies (Figure 1b) (Rimphanitchayakit and Grindley, 1990). The best cocrystal form diffracts X-rays to 2.8 Å resolution and contains a 34 bp site I analog with an overhanging G at each 5′ end. These crystals belong to space group $P2_12_12_1$ and have unit cell dimensions of a = 113.0 Å, b = 157.0 Å, and c = 37.2 Å. Each asymmetric unit contains one resolvase dimer and 34 bp of DNA with 54% (v/v) solvent. The crystal structure was solved by multiple isomorphous replacement using an ethylmercury phosphate (EMP) derivative of a cysteine mutant, S98C, of resolvase (Hatfull et al., 1989), a $HgCl_2$ derivative of a phosphorothioate DNA at specific positions, and an iodouracil derivative of DNA (see Figure 1c; Experimental Procedures) and has been refined to R = 0.235 at 3.0 Å (see Table 1; Figure 2). Every amino acid residue in the resolvase dimer, 34 bp of DNA, and an overhanging G at one of the 5′ ends have been located. Monomers in the resolvase dimer will be referred to as A (residues 1–183) and B (residues 1′–183′). When structural features are common to both monomers, no distinction will be made, and A will be shown as an example. Base pairs are numbered starting from 1 and 1′ at the center of symmetry to 17 at the end where monomer A binds and 17′ at the end where monomer B binds.

Each resolvase monomer has an αβ fold N-terminal catalytic domain (residues 1–120), a 3-helix-bundle C-terminal DNA-binding domain (residues 148–183), and an extended arm region (residues 121–147) that connects the two domains and binds DNA around the minor groove (Figure 3). The two DNA modules form a continuous 34 bp unit with regular base stacking at the junctions. The DNA, mostly in standard B form conformation, is sharply kinked at its center, giving rise to an overall bend of 60° toward the major groove (Figure 3a).

The N-terminal catalytic domain, which has essentially the same structure as that observed in the absence of DNA, dimerizes and interacts with DNA near the crossover point. The dyad-related active site Ser-10 residues are separated by over 30 Å, as in the absence of DNA. The hydroxyl groups of Ser-10 and Ser-10′ are 17 Å and 11 Å away from the phosphorous atoms of the nearest scissile phosphodiester bonds (Figure 3). The centers of the C-terminal DNA-binding domains are separated from one another by 50 Å and from the N-terminal catalytic domains by 47 Å and 55 Å. The DNA-binding domains bind nonsuccessive major grooves on the opposite side of the DNA from the catalytic domains (Figure 3a), as predicted from DNase I footprinting analyses (Abdel-Meguid et al., 1984). The arm region has an extended surface and wraps around the DNA along the minor groove. The resolvase dimer completely encircles the entire 28 bp of site I, burying 5,700 $Å^2$ of protein and DNA solvent-accessible surface upon formation of the complex.

DNA appears to induce and stabilize the folding of the last 63 amino acid residues of resolvase. Most likely, the second half of helix E does not form in the absence of DNA, since the formation of a continuous helix in the crystals of either the N-terminal fragment or intact resolvase in the absence of DNA (Rice and Steitz, 1994a, 1994b) would result in substantial clashes. The formation of this continuous helix E is thus associated with DNA binding, as is also shown to occur when the basic–leucine zipper (bZIP) motif binds to DNA (Weiss et al., 1990).

This complex is strikingly asymmetric. The N- and C-terminal domains of a resolvase dimer are related by different imperfect dyad axes, neither of which coincides with the dyad axis relating the two DNA half sites. Furthermore, the arm region of monomer B contains a straight helix

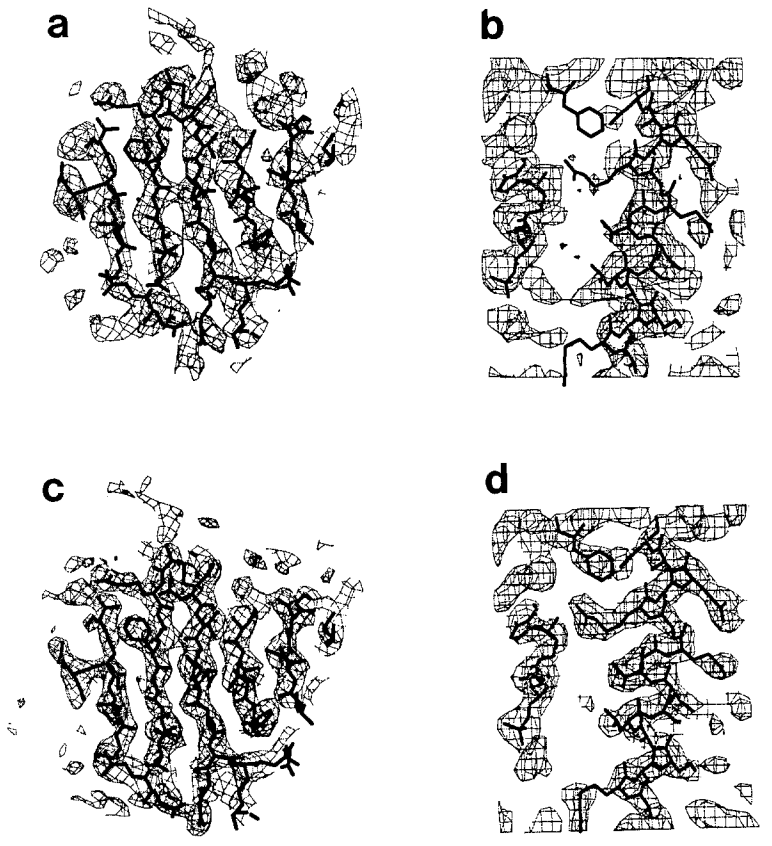

Figure 2. Experimental and Final $2F_o-F_c$ Electron Density Maps

(a) Solvent-flattened MIR map at 3.5 Å resolution contoured at 1σ. Electron density corresponding to the β sheet is shown with the final refined model superimposed.

(b) A 3.0 Å resolution electron density map calculated by using SIGMAA-weighted amplitudes and combined MIR and partial structure phases contoured at 0.8σ. Electron density corresponding to helix E′, which was absent in the refined partial model used in the SIGMAA calculations, is shown with the final refined model superimposed.

(c and d) The final $2F_o-F_c$ map at 3.0 Å resolution and contoured at 1σ. Densities of the same regions as in (a) and (b) are shown, respectively. Figure 2 was made by using O (Jones et al., 1991).

above the DNA minor groove, while in monomer A, this α helix is kinked into the minor groove (Figure 3a). The interactions between resolvase and the DNA are also different in the two subunits. The center of the DNA is closer to monomer B (Figure 3b).

The N-Terminal Catalytic Domain

The N-terminal catalytic domain consists of a five-stranded mixed β sheet surrounded by three α helices on one side and one helix on the other, as described in detail previously (Rice and Steitz, 1994a). Loops 1A and 2B surrounding the active site remain mobile. The dimer interface is formed largely by the pairing of E helices through a hydrophobic ladder and a hydrogen bond between a pair of Glu-118 residues (Figure 4a). Further, the ladder adheres to the edges of the β sheets of each monomer through hydrophobic interactions and connects the hydrophobic cores of the two subunits (Figure 4b). Residues in the hydrophobic core and the dimer interface are quite conserved among members of the resolvase and DNA invertase family (Figure 5a).

Difference–distance matrix analyses (Richards and Kundrot, 1988; A. T. Brünger, X-PLOR version 3.1 [1993]) of five crystal structures of the catalytic domain, three in the absence of DNA (Rice and Steitz, 1994a) and two in the DNA complex, reveal that the largest conformational change in the catalytic domain upon DNA binding occurs at the hinge that links helix E to the rest of the domain, 5E (Figure 6a). Comparisons of the quaternary structures of the catalytic dimer in the presence and absence of DNA show that the hydrophobic interactions between the pair of E helices at the dimer interface do not change very much. However, the remainder of the two catalytic domains shift separately (Figure 6b). In addition, the cavity found between β strands 1 and 3 and helices B and D in the hydrophobic core in resolvase structures (Rice and Steitz, 1994a) becomes closed in monomer A when complexed with DNA.

The Arm Region

The arm region is composed of a helix that extends from the catalytic domain, two extended strands, and two tight turns punctuated by glycine residues. Residues 121–136, which are disordered in crystals of resolvase alone, form the second half of a continuous helix E in the presence of DNA. This half of helix E with large polar side chains first crosses over to the active site of the adjacent dyad-related monomer and then grips DNA in the minor groove (see Figure 3). This extended helix adopts two distinct conformations in this complex with DNA. Helix E′ is straight, whereas helix E in monomer A is kinked by 26° at Asn-127 (Figure 6c). The amino acid sequence surrounding the kink contains no helix-breaking residues except Gly-129, which has reasonably helical dihedral angles (−47°, −50°). The kink seen in helix E but not in E′ contributes to the asymmetric binding of DNA by monomers A and B.

Residues Gly-137 and Gly-141 are invariant in the resolvase family (see Figure 5a), presumably to allow the forma-

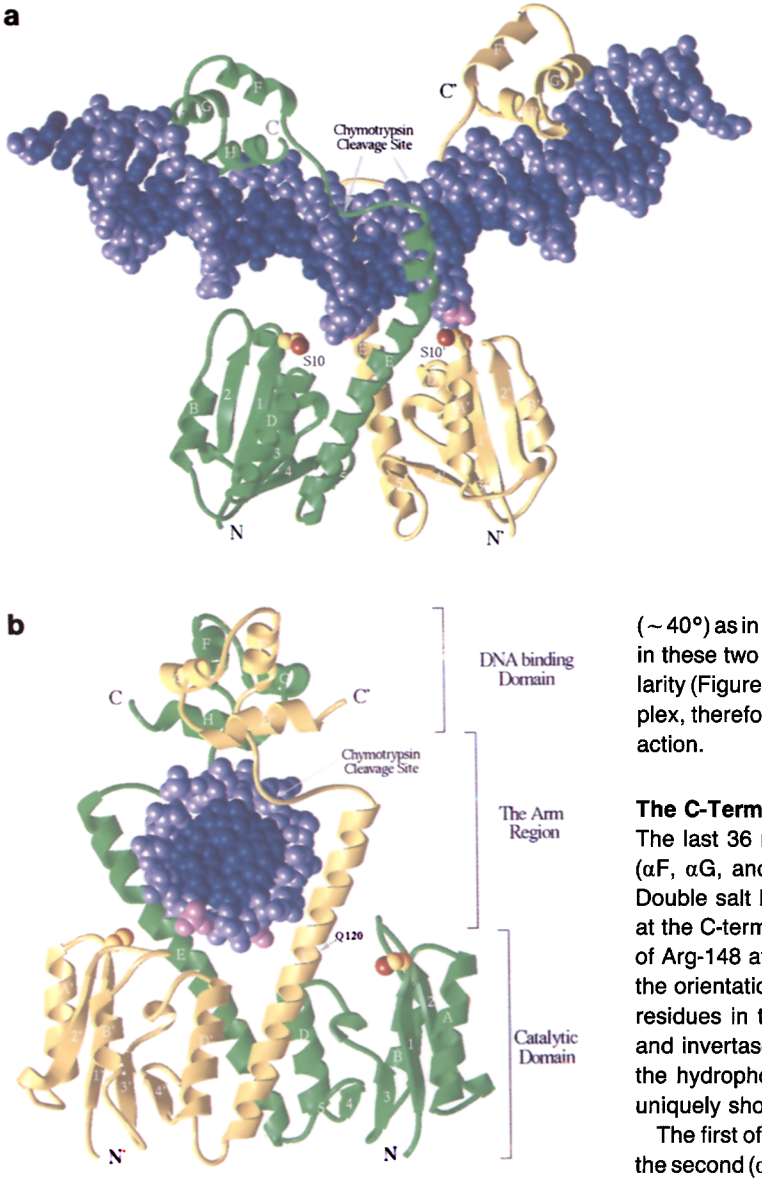

Figure 3. The Structure of the γδ Resolvase–DNA Complex

The resolvase dimer is represented in ribbon diagrams with monomer A in green and monomer B in gold. The active site Ser-10 residues have yellow carbon atoms and red hydroxyl groups. A space-filling model of the DNA has the bases in dark blue and the backbone in light blue. The DNA scissile phosphates are highlighted in magenta. Figures 3, 4, 9, 10, and 11 were made by using graphics program RIBBONS (Carson, 1987).

(a) A view of the resolvase–DNA complex shows that helix E of monomer A is kinked into the minor groove.

(b) A view of resolvase dimer with the central 10 bp of the DNA whose center is closer to the catalytic domain of monomer B.

tion of a specific structure. Helix E terminates at Gly-137 with a sharp turn followed by a short strand (138–140). The 90° elbow formed between helix E and the strand is stabilized by a cluster of hydrophobic residues. The arm again twists at Gly-141 when it plunges into the minor groove of the DNA. The last stretch of the arm is another strand dominated by arginine and lysine. Arg-142 anchors the arm region deep into the DNA minor groove through base-specific interactions.

The pair of E helices is reminiscent of the structures of several bZIP–DNA complexes in which a pair of α helices dimerize and diverge to bind DNA. In the resolvase–DNA complex, E helices have a simple right-handed crossover, resembling a pair of chopsticks, and bind DNA over the minor groove. In contrast, the helices in GCN4 (Ellenberger et al., 1992) form a left-handed coiled coil and bind DNA specifically in the major groove. The crossing angle between the two helices is twice as large in resolvase (~40°) as in GCN4 (~20°). In addition, the pairs of helices in these two complexes approach DNA with opposite polarity (Figure 7). The structure of the resolvase–DNA complex, therefore, reveals a new mode of α helix–DNA interaction.

The C-Terminal DNA-Binding Domain

The last 36 residues of resolvase form a 3-helix bundle (αF, αG, and αH) around a compact hydrophobic core. Double salt bridges between the carboxylate of Glu-181 at the C-terminus of helix αH and the guanidinium group of Arg-148 at the N-terminus of helix αF help to stabilize the orientation of these helices in the bundle. Only three residues in this domain are conserved in the resolvase and invertase family (see Figure 5a), which form part of the hydrophobic core in γδ resolvase. Helix αF in γδ is uniquely shorter at its N-terminus (see Figure 5a).

The first of the three helices (αF) is nearly antiparallel to the second (αG), as seen in the Hin invertase DNA-binding domain (Feng et al., 1994) and an engrailed homeodomain (Kissinger et al., 1990). The second and third helices, αG and αH, form a typical helix-turn-helix (HTH) DNA major groove–binding motif. Residue Asn-169 in the turn of the HTH motif has left-handed ϕ and ψ angles (70° and 15°) the same as the canonical glycine found at this position. In the resolvase family, this position is often occupied by a nonglycine residue (see Figure 5a).

The DNA

To achieve an overall bend angle of 60°, the DNA is distorted by two kinks at the central TATA base pairs while the flanking inverted repeats adopt a mostly B-form conformation, except for the part of the consensus sequence (G13–T14) recognized by the HTH, which bends slightly toward the protein (Figure 8). The two TA steps have base pair roll angles of 34° and 23°, are unstacked with 4.6 Å and 4.3 Å rise per base pair, and are unwound by ~10° (Lavery and Sklenar, 1989). Since the two kinks are not in plane, a writhe of +24° is introduced. Accompanying

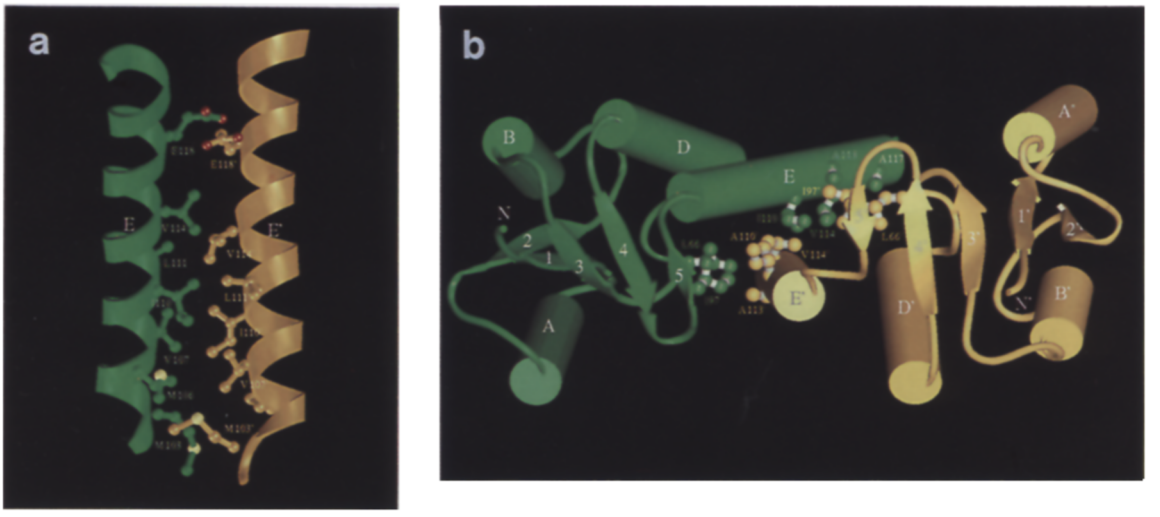

Figure 4. The Resolvase Dimer Interface

(a) The interactions between helices E and E′.

(b) A view down the dyad axis shows that the hydrophobic interactions at the dimer interface extend to the β sheets of the adjacent monomers.

the sharp bend toward the major groove, the minor groove is widened to 7.6 Å from an average of 5.1 Å. The distorted DNA seen in the crystal structure is in good agreement with the kinked and unstacked structure inferred from solution studies of DNA cleavage by MPE–Fe(II) (Hatfull et al., 1987). Since the phosphodiester linkages between the TA steps are also the scissile bonds, the distortions around them may be important for recombination.

Unlike most DNA cocrystal structures, the 34 bp DNA does not stack on DNA from neighboring asymmetric units nor form a pseudocontinuous DNA helix. Instead, the ends of the DNA interact with neighboring resolvase molecules. One end is tightly packed against a symmetry-related resolvase molecule through both hydrophobic and electrostatic interactions. The unpaired G18 form two hydrogen bonds to the guanidinium group of Arg-91′ of a symmetry mate. At this end, the binding to the major groove by resolvase is tighter, and the kink in the DNA between G13 and T14 is more pronounced (Figure 8). The other end of the DNA is less well packed and shows no electron density corresponding to the overhanging G.

Sequence-Specific Interactions in the Major Groove

The 3-helix bundle binds and specifies the outer half of the consensus sequence (T14–G9). Eight hydrogen bonds and salt bridges clamp the C-terminal domain into the major groove (Figure 9a). Main-chain N atoms of Ala-161, Ser-162, and Ala-171 on loops FG and GH as well as the hydroxyl groups of Ser-162, Thr-174, and Tyr-176 form hydrogen bonds to both phosphate backbones; Arg-148 and Lys-177 are salt-bridged to phosphate groups of the DNA.

The base-specific interactions are formed between the side chains of Arg-172, Ser-173, and Tyr-176 and the four DNA base pairs 13–10 (GTCC) (Figure 9a). The guanidinium group of Arg-172 makes hydrogen bonds to the O6 and N7 of G13, an interaction specific for the G·C base pair that is invariant among six occurrences of the conserved recognition sequence in *res* DNA. Mutation of Arg-172 to Leu changes the specificity from G to T (Grindley, 1993). The hydroxyl group of Ser-173 either forms a bifurcated hydrogen bond with the O6 of G10 and G11 or with G10′ alone. Five out of the six recognition sequences have at least one G at positions 10 and 11. The entire phenol ring and Cβ carbon of Tyr-176 interact with the methyl group of T12, another invariant base pair. Hydrophobic interactions also form between the methyl groups of thymidines 14 and 8 and the aliphatic portions of Arg-172 and Lys-177 side chains, respectively.

Sequence-Specific Interactions in the Minor Groove

Interactions between the arm region and minor groove from A8 to T1 seem to impose a requirement for AT- rather than GC-containing sequence, since introduction of the protruding N2 of a guanine would result in a steric clash with this extended arm (Figure 9). Gly-141 fits snugly in the minor groove, with its carbonyl oxygen forming a hydrogen bond to the ribose ring oxygen of T4. Arg-142 has extensive and specific interactions with DNA. Its aliphatic portion is deeply buried in the minor groove and is in van der Waals contact with carbon moieties of the backbone from A4 to T8. Its guanidinium group and main-chain NH make numerous hydrogen bonds to both DNA backbones and to the invariant T·A bases at positions 6 and 7. These interactions, equivalent to those found in the Hin–DNA complex (Feng et al., 1994), and the absolute conservation of Gly-141 and Arg-142 explain why base pairs 4–8 (particularly 6–8) are AT-rich in all DNA consensus sequences recognized by every member in the resolvase and invertase family. Further, the differences in binding of the C-terminal 43 amino acid fragment to mutated DNA consensus sequences provided evidence for minor groove

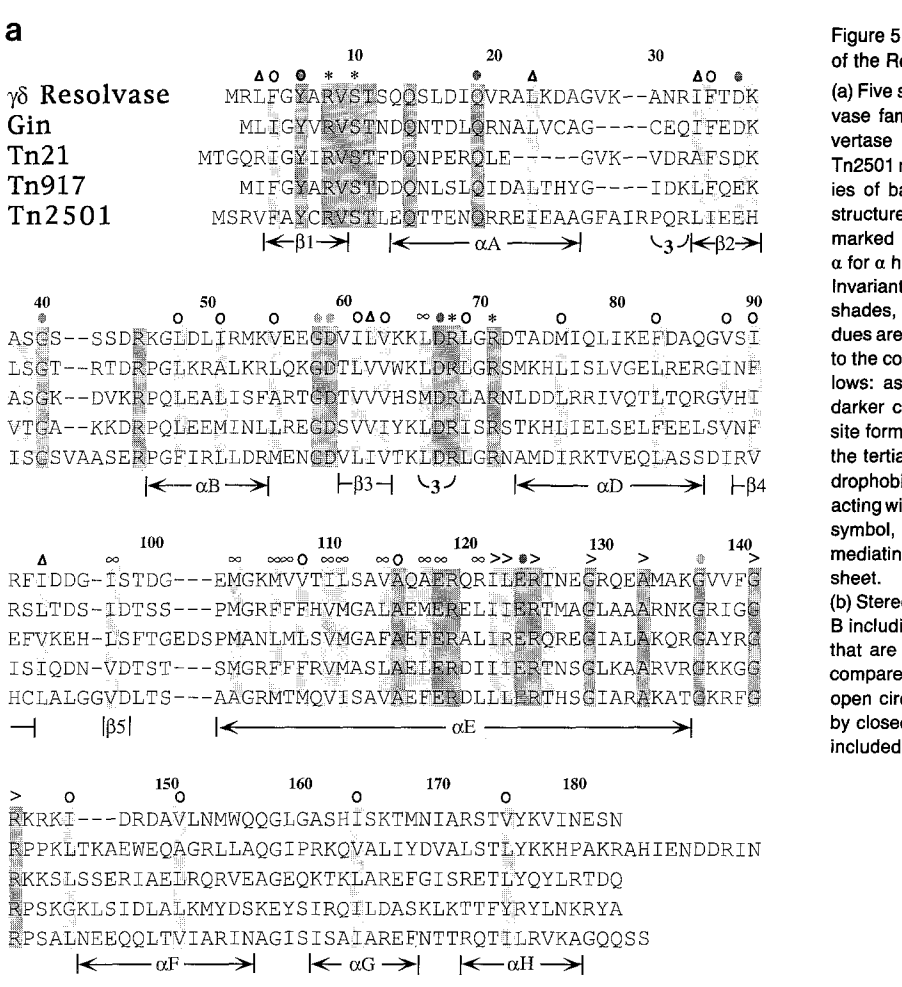

Figure 5. Alignment of Amino Acid Sequences of the Resolvase Family

(a) Five sequences representative of the resolvase family are compared. Gin is a DNA invertase from phage Mu. Tn21, Tn917, and Tn2501 resolvases are from different subfamilies of bacterial transposons. The secondary structures observed in the crystal structure are marked underneath the sequence alignment, α for α helix, β for β strand, and 3 for 3_{10} helix. Invariant residues are highlighted in dark shades, and conservatively substituted residues are in light shades. The function ascribed to the conserved residues are indicated as follows: asterisk, directly involved in catalysis; darker closed circle, important for the active site formation; lighter closed circle, critical for the tertiary structure; open circle, forming hydrophobic cores; greater than symbol, interacting with the DNA in the minor groove; infinity symbol, at the dimer interface; open triangle, mediating interactions between αA and the β sheet.

(b) Stereo tracing of the Cα atoms in monomer B including the side chains of the 24 residues that are invariant among the five sequences compared. Carbon atoms are represented by open circles and oxygen and nitrogen atoms by closed circles. Four central base pairs are included.

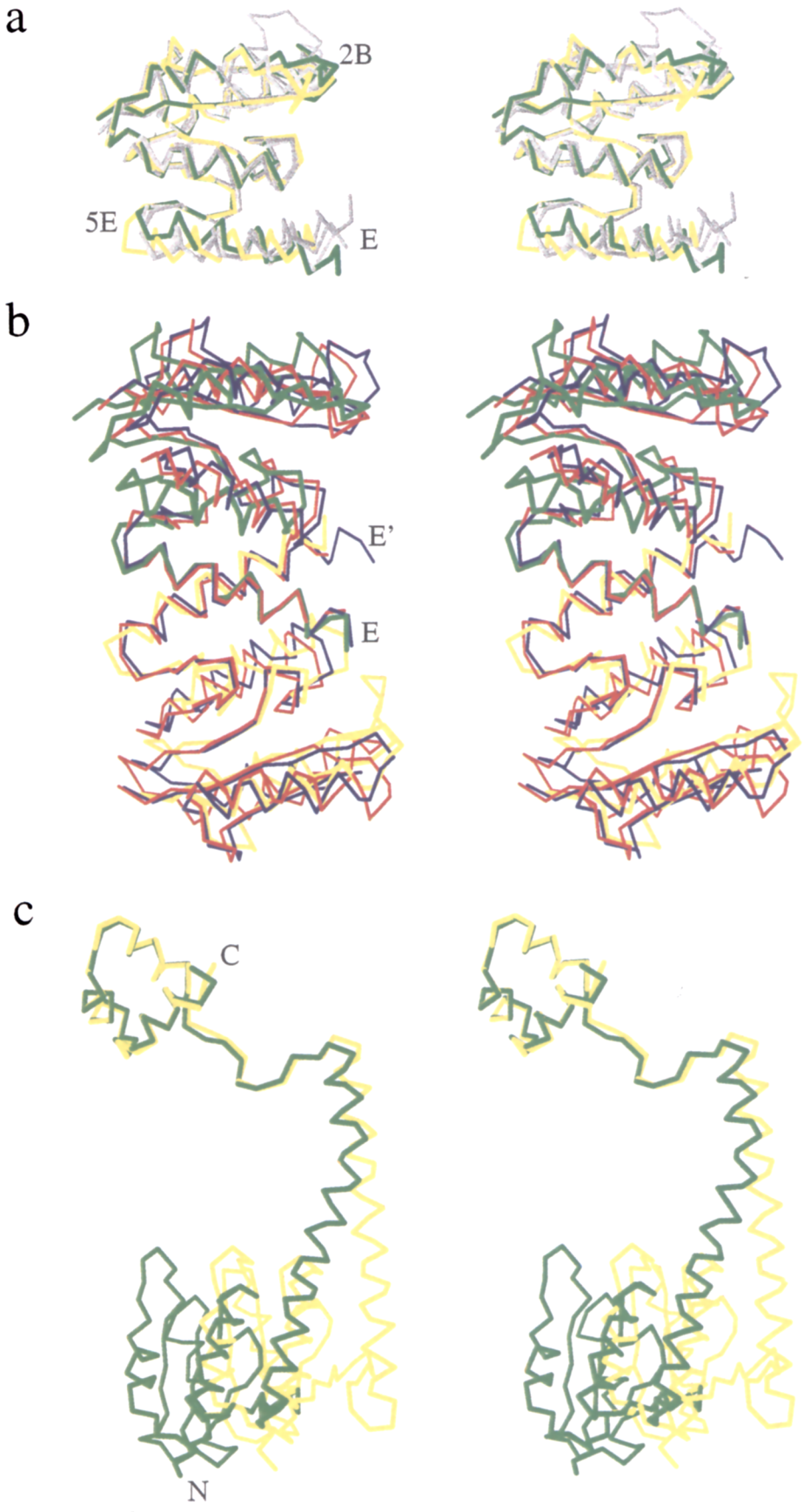

Figure 6. Comparisons of Various Resolvase Structures

(a) Comparison of the five structural determinations of the N-terminal catalytic domain. The two subunits in the DNA complex are shown in green and gold, and the three of the catalytic domain alone are shown in different shades of gray. The main-chain atoms of residues 1–98 except loops 1A and 2B were superimposed (Kabsch, 1976).

(b) Comparison of three structures of the resolvase dimer. The resolvase dimer complexed with DNA is green and gold, while the two different dimers of the catalytic domain are shown in blue (the crystallographic dimer, 33″) and red (the imperfect dimer 12) (Rice and Steitz, 1994a). One E helix from each dimer is superimposed.

(c) Comparison of the two monomers in a resolvase dimer. The same color scheme as in (a) is used. Cα atoms of the C-terminal domain of each monomer are superimposed. Figures 6, 7, and 8 were made using MOLSCRIPT (Kraulis, 1991).

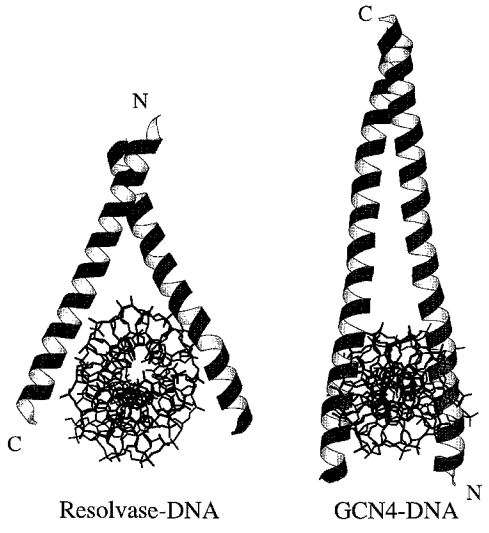

Figure 7. Comparison of Dimerization Helices of Resolvase and GCN4

α helices are represented by ribbons and DNA by ball-and-stick.

interaction with base pairs 5–8 (Rimphanitchayakit and Grindley, 1990). Deletion of Arg-142 in the C-terminal fragment of invertase Hin reduces its affinity for DNA by ~100-fold (Sluka et al., 1990).

The close packing interactions of Thr-126, Arg-130, and Phe-140 with the edges of base pairs in the minor groove and the hydrogen bonds between the guanidinium group of Arg-130 and the N3 atoms of A3 and A4 appear to make monomer A exclude GC-containing sequences between positions 2 and 4 (see Figures 8a and 9b). Mutation of Arg-130 to His interferes with DNA binding (Hughes et al., 1990). Those recombinases that recognize sites having GC at positions 2–5 also have amino acid sequence variation at Thr-126 and Arg-130. The changes may allow these enzymes to recognize the N2 of G in the minor groove. Minor groove recognition may thus be a binary code, either A·T, T·A, or G·C, C·G.

The minor groove interactions made by monomers A and B are asymmetric. The kinked helix E makes more contacts to DNA than the straight helix E′. Arg-125 in monomer A interacts with the H-bond acceptors of A·T at position 1′, while in monomer B neither Arg-130′ nor Arg-125′ interacts with DNA bases (see Figure 8). This asymmetry is consistent with the observation that mutation of one of the central A·T base pairs to G·C had no effect on the affinity of resolvase for site I, but mutation of both A·Ts greatly reduced the binding (Hatfull et al., 1988). The invariant Gly-129 and Ala-133 form close contact with the DNA backbone and may be important in reducing the diameter of the α helix and allowing it to settle into the narrow minor groove. Mutants with larger side chains, such as G129D and A133T, are very defective in DNA binding (Hughes et al., 1990).

Sources of DNA Bending

It is not clear what makes the DNA kink at the central TA base steps. There is no insertion of a large hydrophobic side chain at the kink as seen in the complex of TATA box–binding protein (TBP) and the TATA box (Kim et al., 1993a, 1993b), nor is the minor groove widened in the regions where helices E and E′ interact with the DNA, as observed in a repressor–DNA complex (Schumacher et al., 1994).

The equally strong binding of sites I, II, or III to resolvase implies that there must be structural flexibility to accommodate the different spacings between the inverted repeats. Although the DNA at sites II and III is bent by resolvase binding, the lack of MPE–Fe(II)-hypersensitive cleavage sites indicates that they are not kinked (Hatfull et al., 1987). Mutation of Glu-128 in helix E to Lys made resolvase defective in binding to site III while normal in binding to site I (Hatfull et al., 1987), suggesting that the arm may adapt different structures to stabilize different bends in the DNA through alternative interactions. In accordance with this structural adaptability, the arm region is highly conserved (see Figure 5).

The structure of the arm region is constrained by specific interactions in the minor groove, notably Gly-141 and Arg-142, and by the long connection it has to make between the N- and C-terminal domains. Thr-126 does partially protrude into the wedge formed by the kinked TA step (Figure 8a). Straight DNA bound to resolvase would require the E helices to move further out of the minor groove, thereby decreasing the area of interaction. The kinks in the DNA may also be stabilized by the specific protein dimer interface and the two recognition interfaces between the C-terminal domain of resolvase and the DNA.

The Active Site

Amino acid sequence conservation, the crystal structure of the resolvase–DNA complex, and biochemical characterization of many resolvase mutants indicate that an intact resolvase active site may be dimeric and that the highly conserved Tyr-6, Arg-8, Val-9, Ser-10, Thr-11, Gln-14, Gln-19, Gly-40, Asp-67, Arg-68, Arg-71, Glu-124′, and Arg-125′ (Figure 10) are either important for the formation of the active site or directly involved in catalysis.

Mutations of Tyr-6, Gln-14, Asp-36, Gly-40, or Asp-67 impair recombination while maintaining topoisomerase activity in the presence of Mg^{2+} (Hughes et al., 1990; Leschziner et al., 1995; M. R. Boocock, N. D. F. Grindley, and X. Zhu, personal communication). Tyr-6 contributes its phenol ring to the hydrophobic core and forms a hydrogen bond to the carboxylate oxygen of Asp-36 on strand 2 through its hydroxyl group. The carboxylate group of Asp-36 in turn forms hydrogen bonds to and caps the N-terminus of helix αB. Thus, Tyr-6 and Asp-36 seem to be essential for maintaining the tertiary structure around the active site, although not directly involved in DNA cleavage and religation. The other category of mutations includes Arg-8 to Gln and Arg-68 or Arg-71 to His, which virtually abolish DNA cleavage, as do Ser-10 mutants (Hatfull and Grindley, 1988; Hughes et al., 1990; M. R. Boocock and N. D. F. Grindley, personal communication). Arg-71′ is directly hydrogen bonded to the DNA backbone of A2′, and Arg-8 and Arg-68 are within 5 Å of Ser-10. These arginines may serve to position the scissile bonds and stabilize the cleavage intermediate.

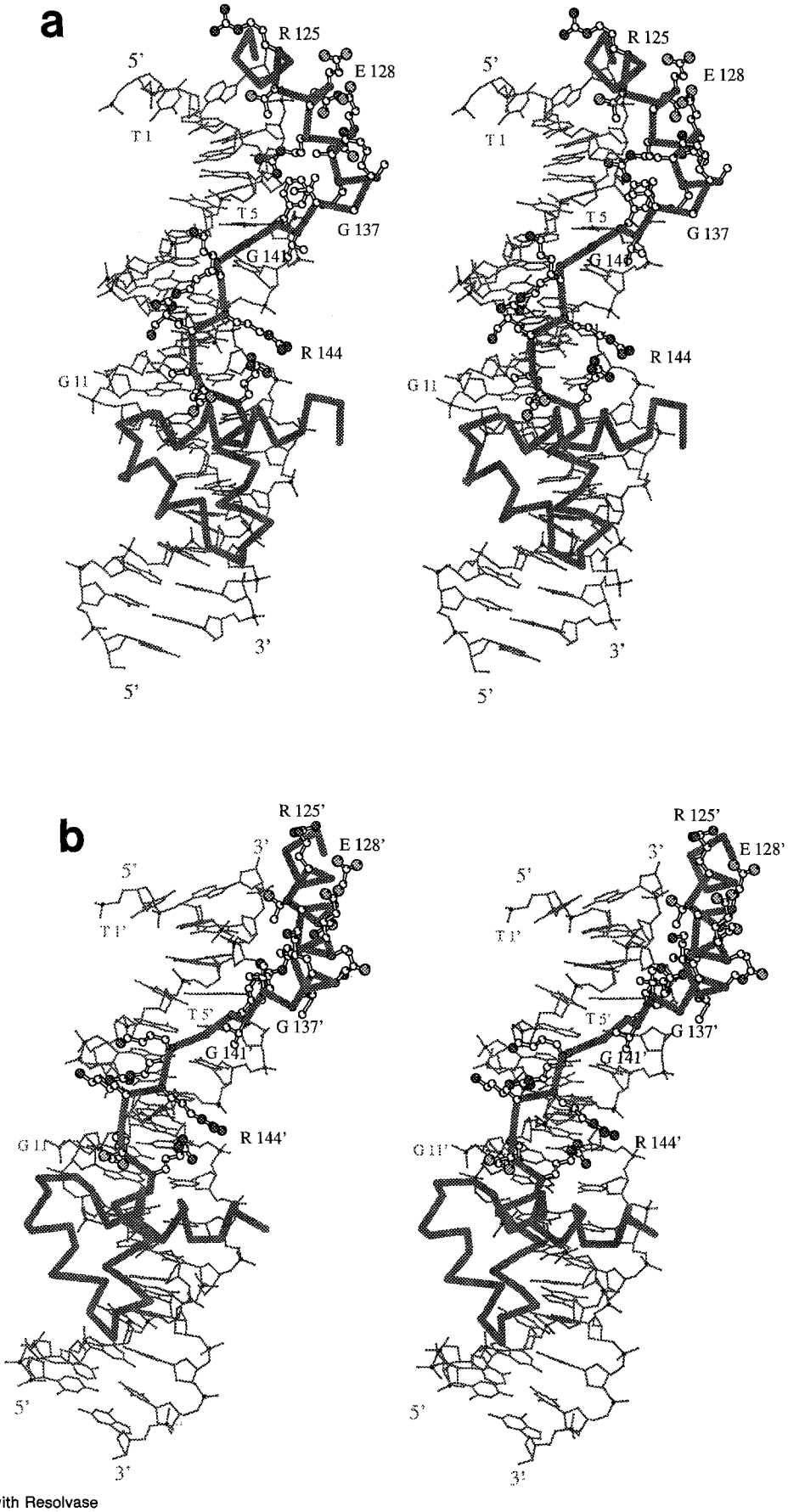

Figure 8. The DNA in Complex with Resolvase

(a and b) Stereo drawings of each half of the DNA bound by the C-terminal 63 amino acid residues of resolvase, which are shown as Cα trace with side chains of residues between 125 and 148 displayed.

DNA binding and cleavage by resolvase have been inferred to occur in *cis*: a resolvase dimer cleaves the site I that it binds to (Dröge et al., 1990; Grindley, 1993); a monomer binds and cleaves the same half of site I (M. R. Boocock and N. D. F. Grindley, personal communication). In this crystal structure, Ser-10 is much closer than Ser-10′ to the scissile bond on the half binding site to which monomer A binds. However, the proximity of helix E to the active

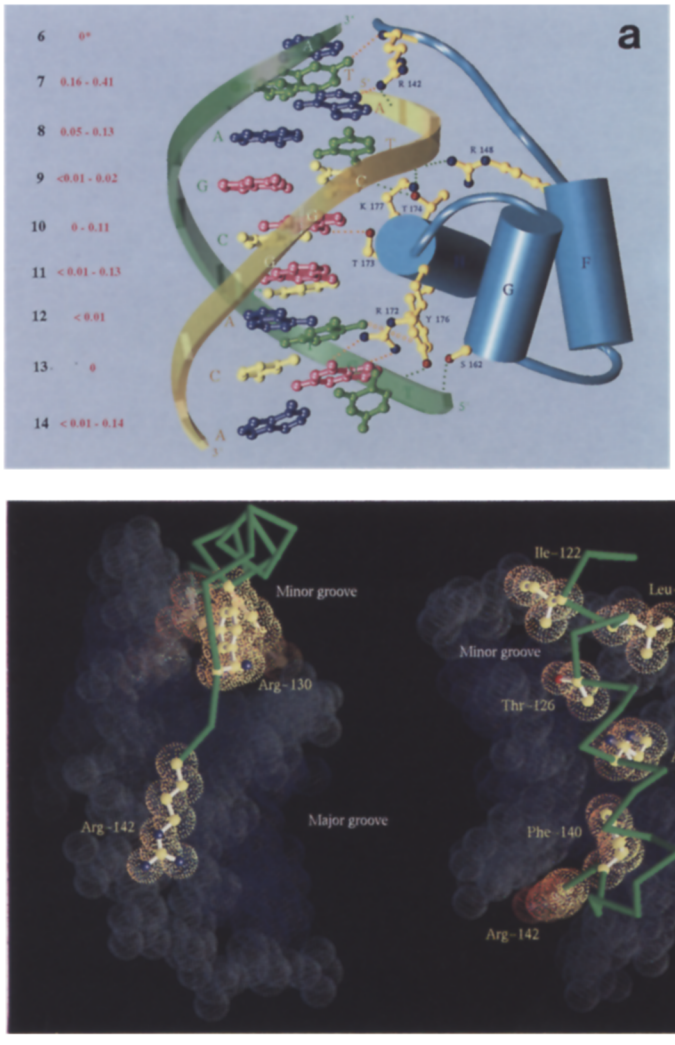

Figure 9. The Interactions between Resolvase and the DNA

(a) The C-terminal fragment of resolvase (residues 141–183) makes sequence-specific interactions with the DNA bases in the adjacent major and minor grooves. The α helices are represented as cylinders and the extended strand and loops as tubes. DNA backbones are represented as green and gold ribbons. DNA bases are represented in different colors: A, blue; C, yellow; G, pink; and T, green. The contacts made by resolvase to the DNA are color and shape coded: hydrogen bonds to the DNA bases are shown as dotted orange lines; hydrogen bonds to the sugar–phosphate backbones as dotted olive lines; and hydrophobic contact as a string of orange bubbles. The two columns on the left are the base pair numbers, the same as in Figure 1b, and the fractional binding affinity of the DNA for resolvase when individual base of the consensus sequence is mutated to the three alternatives, except for base pair 6, where zero affinity results from mutation of A·T to G·C (Rimphanitchayakit and Grindley, 1990).

(b) Minor groove interactions by the arm region. Base pairs 1–8 are shown in atomic surface, with backbones and bases in lighter and darker blues. The arm region is shown in green Cα trace; side chains in close and specific contact with bases are presented.

site of the adjacent subunit (Glu-124 to Ser-10′ and Arg-68′) (Figure 10) and to the DNA scissile bond (Arg-125 to T1′), sequence conservation of Glu-124 and Arg-125, and the requirement of a native dimer interface indicate that a single active site may be composed of residues from both monomers. Changes of the bulkiness or the polarity on the dimer interface by mutations, such as I110T, I110W, or E118K, drastically affect both recombinase and topoisomerase activities (Hatfull et al., 1987; Hughes et al., 1993). Thus, the precise position of helix E relative to the next monomer appears to be critical for the catalysis. Interestingly, mutations affecting the helix to β-sheet interaction at the dimer interface in Gin invertase, M114V (which is equivalent to Ala-117 in γδ) or H106Y (Thr-109 in γδ), make Gin much more reactive and independent of the accessory protein FIS (Klippel et al., 1993).

A Sequential Single-Strand Cleavage Mechanism

Double-strand rather than single-strand cleavage at each crossover point is normally observed. The crystallographic and biochemical identification of the catalytic resolvase dimer, however, has presented a dilemma: the two active site Ser-10 residues in the catalytic dimer are more than 30 Å apart, whereas the two scissile bonds at a crossover point are only 13 Å apart in a standard B-form DNA. How then can the double-strand cleavages happen simultaneously? Neither the possibility that the dimer interface changes, perhaps by the pair of E helices moving in a scissors-like fashion to bring the two serine residues closer (Rice and Steitz, 1994b), nor the possibility that the DNA might become sufficiently distorted to contact both serine residues simultaneously has been observed in the current resolvase–DNA complex. An attempt to model a resolvase–DNA complex with a more distorted DNA structure taken from the complex of TBP and TATA box DNA (Kim et al., 1993b) made the scissile bonds 22 Å apart but no closer to the active site serine residues.

That the resolvase–DNA complex is asymmetric, with the central TATA base pairs closer to the Ser-10′ and monomer B than to Ser-10 and monomer A (Figure 3b), raises the possibility that cleavage occurs first at one scissile bond and then at the other. The extent of structural asymmetry is likely to be even greater in a complex with the asymmetric native site I sequence and in the synaptosome, where the right half of site I is followed by sites II and III and the left half is adjacent to the boundary of

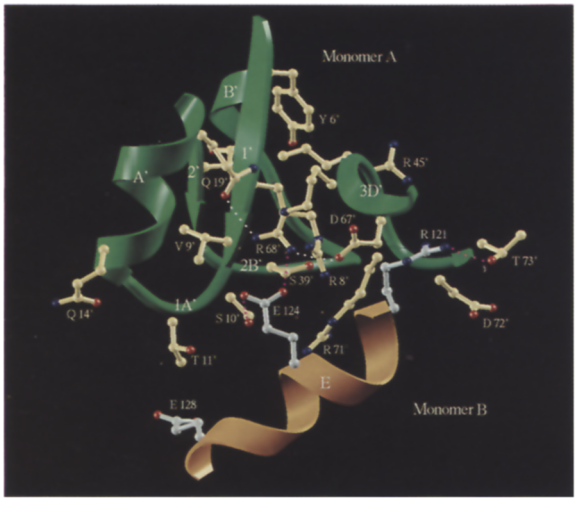

Figure 10. The Active Site

Residues around active site Ser-10′ are shown as ball-and-stick representations. The backbones of monomers A (gold) and B (green) are represented as ribbon diagrams. Carbon atoms of monomer B are colored yellow, while those of monomer A are white. Nitrogen atoms are blue and oxygen atoms red. Hydrogen bonds between two monomers are colored purple, and those within monomer B are white.

res DNA. Earlier experiments on mutations of DNA at the crossover point (Falvey et al., 1988) and recent studies on heterodimers of active and inactive resolvase mutants (M. R. Boocock and N. D. F. Grindley, personal communication) have yielded the following two interesting results: first, that single-strand nicking is observed, and second, that the top strand is cleaved more frequently. We thus suggest the possibility of coordinated but sequential single-strand cleavages in site I that may be assisted by sites II and III in the synaptosome.

Although this cocrystal structure is an inactive complex where the active site Ser-10 residues are on a flexible loop and far away from scissile phosphodiester bonds, it has shed light on the conformational changes that may lead to an active recombination complex. First, the variable structures of hinge 5E suggest that it can serve as a pivotal point to swing DNA relative to the N-terminal catalytic domain (see Figures 3b and 6b). Second, the adaptability in the resolvase arm region, the bendability of DNA at the crossover point, and the smooth resolvase–DNA interface around the central minor groove (see Figures 6c, 8, and 9b) suggest that more distortion in both resolvase and DNA as well as a rocking motion of the DNA relative to resolvase can take place. In a synaptosome, additional protein–protein and protein–DNA interactions may induce an even more asymmetric interaction between resolvase and site I and bring one scissile bond closer to one Ser-10 residue. Presumably, once the DNA is in, the active site residues on the flexible loops will be more ordered and poised for catalysis.

Formation of the Synaptosome

Some insights into the structure of the synaptosome may be gained from the resolvase–DNA complex, the protein–protein contacts observed in crystals without DNA (Rice and Steitz, 1994a, 1994b), and mutagenesis and biochemical studies designed to assess which of the observed protein–protein contacts are relevant to recombination (Hughes et al., 1990, 1993). Interdimer interactions that were evident in the two crystal forms of resolvase alone resulted in a consistent tetramer of catalytic dimers with D2 symmetry. Mutations of residues that form one of these interdimer interfaces (called the 2–3′ interface) disrupt the cooperative interactions between dimers bound to *res* DNA at sites II and III and abolish synapsis and recombination. Rice and Steitz (1994b) hypothesized that this interdimer interface mediates the association of resolvase dimers bound to sites II and III with a 34.5 bp center-to-center separation on the same *res* DNA. Further, the tetramer of dimers was proposed to synapse sites II and III of two *res* DNAs. Although there are no dyad axis–related interactions between resolvase dimers in the site I DNA cocrystal, the catalytic domains of this complex were superimposed on the corresponding domains in the tetramer of dimers that occurs in the crystal of the N-terminal fragment. With the complex oriented this way, the DNA-binding domains all point outward from the catalytic domains (Figure 11a). Interestingly, the DNAs bound to the two resolvase dimers related by a 2–3′ interface are nearly continuous (Figure 11b), as hypothesized earlier (Rice and Steitz, 1994b). Although the distance between sites II and III matches perfectly with the site I analog in the resolvase–DNA cocrystal, there must be changes in the structure when resolvase is complexed with sites II and III because of the different spacing between inverted repeats in each binding site and their asymmetric surroundings (see Figure 1b).

The relative position of the two resolvase dimers bound to site I in the synaptosome remains a matter of considerable conjecture. Assuming that the dyad axes are likely to be coincident, two arrangements of the site I complexes in the synaptosome are possible. Similar to what Rice and Steitz (1994b) postulated, the two bent DNAs may contact in a handshake fashion and the major grooves of the two crossover points face each other (Figure 11c). In this orientation, the conserved residues on the arm regions of resolvase are close to each other and may explain the observed coordinated cleavages of both site I DNAs in the synaptosome. The relative proximity of the two crossover points could facilitate DNA strand exchange. The other possibility is that the interdimer contact is mediated by the surface of the resolvase N-terminal catalytic domain distal to the DNA-binding surface (Figure 11d). In this case, the two crossover points in the DNAs involved in strand exchange and rejoining are separated by over 50 Å and both of the resolvase dimers.

Strand Exchange

The major question remaining to be answered is how DNA strand exchange takes place in a synaptosome. Two general types of models have been proposed. The resolvase subunit rotation model postulates that two resolvase dimers dissociate, switch partners, and reassociate accompanying DNA cleavage, strand exchange, and religation (Stark et al., 1991; Stark and Boocock, 1994). In this

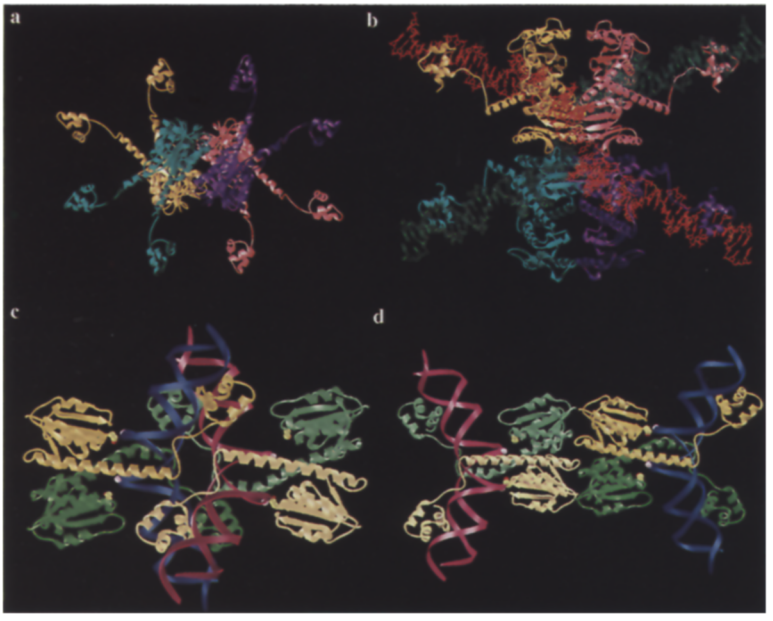

Figure 11. Possible Interactions in the Synaptosome

(a) The intact resolvase dimer structure from the complex was superimposed onto the tetramer of dimers found in the crystals of the N-terminal catalytic domain (Rice and Steitz, 1994b). Each resolvase dimer is shown in a distinct color: pink, purple, aqua, or yellow. Yellow and purple dimers are held together by 23′-type interdimer interface (Sanderson et al., 1990); so are pink and aqua dimers.

(b) An orthogonal view from (a) with DNAs shown. The two DNAs in the front are colored red, and the two in the back are colored green. DNAs in the same color are proposed to be the adjacent sites II and III in *res* and are seen to be almost continuous.

(c and d) Two opposite ways of assembling two site I complexes in the synaptosome, assuming their dyad axes are coincident: (c), with the DNAs inside between the two protein dimers; (d), with the DNAs outside. One resolvase dimer is shown in green and golden ribbon diagrams and complexed with blue DNA; the other dimer is in lighter colors and complexed with purple DNA. The DNA scissile bonds are highlighted in pink.

model, there are no protein–protein interactions to hold the cleaved DNA together during strand rotation. A second model postulates that the two duplexes to be recombined are held in close proximity surrounded by two resolvase dimers and that recombination occurs by distortions and conformational changes in the DNA at the crossover points. Rice and Steitz (1994b) hypothesized that each DNA duplex was unwound by 180° upon binding to the protein, which is not observed in the present crystal structure. A new possibility consistent with the structure presented here is that the DNA becomes partially denatured around the crossover point following the cleavage and that the newly formed 3′ ends of DNA cross over to religate. How the protein might facilitate such a strand exchange is not obvious; however, it would presumably require substantially smaller changes in structure than are necessary in the subunit rotation model. To address this central issue, resolvase has been cocrystallized with *res* DNA (W. Y. and T. A. S., unpublished data), and a FIS-independent mutant of GIN has been cocrystallized with *gix* DNA (S. Bellon and T. A. S., unpublished data). Determination of one or both of these cocrystal structures should provide direct insights into the mechanism of DNA strand exchange.

Experimental Procedures

Crystallization of the γδ Resolvase–DNA Complex

Overexpression vectors derived from plasmid mGH285 containing the genes coding for native or mutant γδ resolvase were freshly transformed into E. coli strain AR120, and resolvase was overexpressed and purified according to the published procedure (Hatfull et al., 1989). A DEAE–cellulose column was added before the CM–Sepharose column to remove DNAs. Protease inhibitors such as phenylmethylsulfonyl fluoride, benzamidine, leupeptin, and aprotinin were used in purification. Oligonucleotides were purified on high pressure liquid chromatography reverse phase columns with the trityl protection group on and again after detritylation by acetic acid. The best diffracting crystals were grown by the hanging-drop vapor diffusion method at room temperature. The initial components of 2–6 μl hanging drops were as follows: 0.36 mM resolvase monomer, 0.72 mM DNA modular duplex, 0.2 M ammonium sulfate, 2.5% ethylene glycol, 0.5 mM EDTA, 10 mM Tris buffer (pH 8.0), 50 mM MES buffer (pH 6.0), and 15% PEG 3350. The reservoir contained 0.2 M ammonium sulfate, 5% ethylene glycol, 100 mM MES buffer (pH 6.0), and 30% PEG 3350. Starting from microseeds, rod-like crystals grew to a maximal size of 0.12 × 0.08 × 0.6 mm within 1–2 weeks. Crystals were harvested after they reached the maximal size and stored in a stabilization solution containing 0.2 M ammonium sulfate, 5% ethylene glycol, 100 mM sodium acetate buffer (pH 5.5), and 32% PEG 3350.

Isomorphous Derivatives

Isomorphous derivatives were prepared by using either cysteine mutants of resolvase K65C, D72C, or S98C (Hatfull et al., 1989) or phosphorothioate DNA (Figure 1c). Cocrystals of each of these modified components and their native partners were grown under similar conditions as the native complex. The isomorphous mercurial derivatives were made by soaking the cocrystals of a cysteine mutant in the stabilization solution containing 0.6 mM EMP and those of phosphorothioate in 0.1 mM $HgCl_2$ for over 24 hr. Iodouracil substitutions of thymidine at five positions were also tried. Four of them yielded cocrystals, only one of which was large enough for diffraction data collection (Figure 1c).

Data Collection and Processing

All crystals were flash frozen directly in a N_2 stream at −160°C after being transferred to a cryosolvent containing 10% ethylene glycol in addition to the other components of the stabilization solution for 10–20 min. One native and three derivative data sets were collected on an R-axis IPII system, which was mounted on a Rigaku RU200 generator with a mirror optical device designed in-house. Data sets were processed by using DENZO and SCALEPACK (Otwinowski, 1993). Although these crystals diffracted nearly isotropically to 2.8 Å, the effective resolution limit of the most complete data set collected from the native crystal was 3.0 Å (Table 1). Derivative data sets were scaled to the native one by local scaling and anisotropic B scaling.

Structure Determination

Molecular replacement (MR) using the dimeric resolvase structure of the N-terminal 120 amino acids (Rice and Steitz, 1994a) as the search model was successfully carried out with X-PLOR (version 3.1 [1993]; A. T. Brünger, Howard Hughes Medical Institute and Department of Molecular Biophysics and Biochemistry, Yale University, New Haven,

Table 1. Summary of Crystallographic Data

Data Collection	Native	S98C–EMP	Thioate–DNA–$HgCl_2$	IdU7
Diffraction limits (Å)	3.0	3.0	2.8	2.8
Observed reflections	13255	9920	13490	14378
Completeness (%)	94.2	69.7	78.6	83.7
R_{sym}[a] (%)	7.7	11.9	7.1	8.3
Isomorphous difference[b] (%)	–	19.7	11.6	21.2

MIR Phasing Statistics	Resolution Shells (Å)							
	12.7	8.8	6.8	5.5	4.6	4.0	3.5	Total
S98C–EMP								
Number of reflections	158	368	664	1033	1419	1775	2051	7468
Phasing power[c]	2.01	1.67	1.68	1.51	1.08	0.80	0.60	1.06
Thioate DNA–$HgCl_2$								
Number of reflections	176	402	690	1070	1482	1893	2190	7903
Phasing power[c]	2.29	1.57	1.10	0.75	0.34	0.15	0.07	0.75
Iodinated DNA (IU7)								
Number of reflections	166	402	687	1071	1509	2073	2625	8533
Phasing power[c]	0.24	0.39	0.52	0.58	0.47	0.39	0.41	0.38
Mean figure of merit[d]	0.73	0.64	0.60	0.54	0.40	0.30	0.24	0.38

Refinement Statistics	
Resolution range	10.0–3.0
R factor[e]	0.235
Reflections with $\|F_o\| > 2\sigma(\|F_o\|)$ (completeness)	12130 (90.2%)
Total nonhydrogen atoms	4255
Water molecules	29
rms deviations from ideality	
bond length (Å)	0.012
bond angle (degrees)	1.252
Averaged B value for main-chain atoms (Å^2) (rms, 1.11)	24.33
Averaged B value for DNA and side-chain atoms (Å^2) (rms, 2.12)	29.05

[a] $R_{sym} = \Sigma_h\Sigma_i|I_{hi} - \langle I_h\rangle| / \Sigma\langle I_h\rangle$ where $\langle I_h\rangle$ is the mean intensity of h reflection and I_{hi} is i^{th} observation of h reflection.
[b] Isomorphous difference $= \Sigma|F_{ph} - F_p| / \Sigma|F_p|$ where F_p and F_{ph} are observed structure amplitudes of the native and heavy atom derivative complexes.
[c] Phasing power $= \Sigma |F_h| / [||F_p|\exp(i\Phi)\varphi + F_h| - |F_{ph}|]$ where F_h is the calculated structure factor of the heavy atoms and Φ is the calculated phase of the native complex.
[d] Figure of merit $= \int P(\Phi)\exp(i\Phi)d\Phi \int P(\Phi)d\Phi$ where P is the probability distribution of the phase angle Φ.
[e] $R = \Sigma|F_o - F_c| / \Sigma|F_o|$ where F_o and F_c are the observed and calculated structure amplitudes of the native complex.

CT) when a phased translation search (Fujinaga and Read, 1987) was incorporated. Diffraction data between 10 Å and 4.5 Å spacing and phases derived from a single isomorphous derivative of S98C EMP were used. The correct rotation solution turned out to be the thirtieth peak in the rotation function and the fifth peak after PC refinement. The correct solution from the phased translation search gave a peak of 10.8σ versus peaks of 4–5σ for the incorrect ones. No translation solution was found in Patterson space even with the correct rotation solution.

The heavy atom positions in the S98C EMP and phosphorothioate-$HgCl_2$ derivatives were determined independently from difference Patterson maps. The iodine positions were determined by the difference Fourier method. The MR solution did not contribute to phasing, but it was used to cross-examine the multiple isomorphous replacement (MIR) solutions. Heavy atom parameters were refined by using the original INPHARE and PHARE (Otwinowski, 1991). Phase statistics are shown in Table 1. Because of the presence of both stereoisomers of phosphorothioate (Figure 1c), two alternative $HgCl_2$ sites were identified for each phosphorothioate. Their occupancies relative to the EMP in S98C resolvase were a little less than 0.5. A detailed description of the use of phosphorothioate as a general vehicle for making heavy-atom derivatives in nucleic acids will be published elsewhere.

The electron density maps calculated by using MIR phases were discontinuous even at 5.5 Å resolution. Averaging by 2-fold lowered the effective resolution, owing to the conformational and thermodynamic differences between the two subunits in each asymmetric unit. Solvent flattening by a modification of the procedure of Wang (1985) implemented in the CCP4 package dramatically improved connectivity of the experimental map, especially at higher resolution (Figure 2a). This map enabled us to build the initial model of the N- and C-terminal domains and the central 28 bp in the DNA by using the program FRODO (Jones, 1978). Density corresponding to ~30 residues in the arm region in each monomer was missing, and the ends of the DNA were not well defined.

We refined the initial model against native diffraction data between 8 Å and 3 Å reciprocal lattice spacings with a 2σ cut-off and reduced the R value to 0.315 by sequential use of RIGID, PREPSTAGE, SLOW-COOL, and BGROUP refinement protocols in X-PLOR (A. T. Brünger). SIGMAA (Read, 1986) in the CCP4 package was used to combine the experimentally determined structure factors with those calculated from the refined partial model. Low resolution reflections (25.0–8.0 Å) were included in the weight calculation and used similarly to the free R calculation as an indicator for the quality of refinement (A. T. Brünger). A SIGMAA-weighted $2F_o–F_c$ map contoured at 0.8σ revealed the density for the arm region (Figure 2b). With many cycles of refinement by X-PLOR, phase combination by SIGMAA, and model refitting manu-

ally, we built the entire polypeptide chain and fit the ends of DNA. After the R value went below 25%, we included more reflections (10–3 Å) in refinement and refined the individual isotropic B factors for each atom with very tight restraints imposed on atoms either directly or indirectly bonded. We also included 29 water molecules. The refinement statistics are shown in Table 1. The coordinates of this complex have been deposited with Protein Data Bank under the ID code of 1GDT.

Acknowledgments

We thank N. Grindley, M. Boocock, and P. Rice for stimulating discussions, and T. Fischmann, J. Friedman, J. Jaeger, D. Jeruzalmi, and J. Wang for technical help. We appreciate the critical reading of the manuscript by N. Grindley, M. Boocock, and S. Smerdon. This research was supported by National Institutes of Health grant GM22778 to T. A. S.

Received March 20, 1995; revised May 22, 1995.

References

Abdel-Meguid, S. S., Grindley, N. D. F., Templeton, N. S., and Steitz, T. A. (1984). Cleavage of the site-specific recombination protein γδ resolvase: the smaller of two fragments binds DNA specifically. Proc. Natl. Acad. Sci. USA *81*, 2001–2005.

Bednarz, A. L., Boocock, M. R., and Sherratt, D. J. (1990). Determinants of correct *res* site alignment in site-specific recombination by Tn3 resolvase. Genes Dev. *4*, 2366–2375.

Benjamin, H. W., and Cozzarelli, N. R. (1988). Isolation and characterization of the Tn3 resolvase synaptic intermediate. EMBO J. *7*, 1897–1904.

Carson, M. (1987). Ribbon models of macromolecules. J. Mol. Graphics *5*, 103–106.

Ellenberger, T. E., Brandl, C. J., Struhl, K., and Harrison, S. C. (1992). The GCN4 basic region leucine zipper binds DNA as a dimer of uninterrupted α helices: crystal structure of the protein–DNA complex. Cell *71*, 1223–1237.

Dröge, P., Hatfull, G. F., Grindley, N. D. F., and Cozzarelli, N. R. (1990). The two functional domains of γδ resolvase act on the same recombination site: implications for the mechanism of strand exchange. Proc. Natl. Acad. Sci. USA *87*, 5336–5340.

Falvey, E., Hatfull, G. F., and Grindley, N. D. F. (1988). Uncoupling of the recombination and topoisomerase activities of the γδ resolvase by a mutation at the crossover point. Nature *332*, 861–863.

Feng, J. A., Johnson, R. C., and Dickerson, R. E. (1994). Hin recombinase bound to DNA: the origin of specificity in major and minor groove interactions. Science *263*, 348–355.

Fujinaga, M., and Read, R. J. (1987). Experiences with a new translation-function program. J. Appl. Cryst. *20*, 517–521.

Grindley, N. D. F. (1993). Analysis of a nucleoprotein complex: the synaptosome of γδ resolvase. Science *262*, 738–740.

Grindley, N. G. F. (1994). Resolvase-mediated site-specific recombination. Nucl. Acids Mol. Biol. *8*, 236–267.

Grindley, N. D. F., Lauth, M. R., Wells, R. G., Wityk, R. J., Salvo, J. J., and Reed, R. R. (1982). Transposon-mediated site-specific recombination: identification of three binding sites for resolvase at the *res* sites of γδ and Tn3. Cell *30*, 19–27.

Hatfull, G. F., and Grindley, N. D. F. (1988). Resolvases and DNA-invertases: a family of enzymes active in site-specific recombination. In Genetic Recombination, R. Kucherlaphati and G. R. Smith, eds. (Washington, D. C.: American Society for Microbiology), pp. 357–396.

Hatfull, G. F., Noble, S. M., and Grindley, N. D. F. (1987). The γδ resolvase induces an unusual DNA structure at the recombinational crossover point. Cell *49*, 103–110.

Hatfull, G. F., Salvo, J. J., Falvey, E. E., Rimphanitchayakit, V., and Grindley, N. D. F. (1988). Site-specific recombination by the γδ resolvase. Symp. Soc. Gen. Microbiol. *43*, 149–181.

Hatfull, G. F., Sanderson, M. R., Freemont, P. S., Raccuia, P. R., Grindley, N. D. F., and Steitz, T. A. (1989). Preparation of heavy-atom derivatives using site-directed mutagenesis. J. Mol. Biol. *208*, 661–667.

Hughes, R. E., Hatfull, G. F., Rice, P. A., Steitz, T. A., and Grindley, N. D. F. (1990). Cooperativity mutants of the γδ resolvase identify an essential interdimer interaction. Cell *63*, 1331–1338.

Hughes, R. E., Rice, P. A., Steitz, T. A., and Grindley, N. D. F. (1993). Protein–protein interactions directing resolvase site-specific recombination: a structure-function analysis. EMBO J. *12*, 1447–1458.

Jones, T. A. (1978). A graphics model building and refinement system for macromolecules. J. Appl. Cryst. *11*, 268–272.

Jones, T. A., Zou, J.-Y., Cowan, S. W., and Kjeldgaard, M. (1991). Improved methods for building protein models in electron density maps and the location of errors in these models. Acta Cryst. *A47*, 110–119.

Kabsch, W. (1976). A solution for the best rotation to relate two sets of vectors. Acta Cryst. *A32*, 922–923.

Kim, J. L., Nikolov, D. B., and Burley, S. K. (1993a). Co-crystal structure of TBP recognizing the minor groove of a TATA element. Nature *365*, 520–527.

Kim, Y. C., Geiger, J. H., Hahn, S., and Sigler, P. B. (1993b). Crystal structure of a yeast TBP/TATA-box complex. Nature *365*, 512–520.

Kissinger, C. R., Liu, B., Martin-Blanco, E., Kornberg, T. B., and Pabo, C. O. (1990). Crystal structure of an engrailed homeodomain–DNA complex at 2.8 Å resolution: a framework for understanding homeodomain–DNA interactions. Cell *63*, 579–590.

Klippel, A., Kanaar, R., Kahmann, R., and Cozzarelli, N. R. (1993). Analysis of strand exchange and DNA binding of enhancer-independent Gin recombinase mutants. EMBO J. *12*, 1047–1057.

Krasnow, M. A., and Cozzarelli, N. R. (1983). Site-specific relaxation and recombination by the Tn3 resolvase: recognition of the DNA path between oriented *res* sites. Cell *32*, 1313–1324.

Kraulis, P. J. (1991). MOLSCRIPT: a program to produce both detailed and schematic plots of protein structures. J. Appl. Cryst. *24*, 946–950.

Lavery, R., and Sklenar, H. (1989). Defining the structure of irregular nucleic acids: conventions and principles. J. Biomol. Struct. Dyn. *6*, 655–667.

Leschziner, A. E., Boocock, M. R., and Grindley, N. D. F. (1995). The tyrosine-6 hydroxyl of γδ-resolvase is not required for the DNA cleavage and rejoining reactions. J. Mol. Microbiol. *15*, 865–870.

Newman, B. J., and Grindley, N. D. F. (1984). Mutants of the γδ resolvase: a genetic analysis of the recombination function. Cell *38*, 463–469.

Otwinowski, Z. (1991). ML-PHARE. In Isomorphous Replacement and Anomalous Scattering, W. Wolf, P. R. Evan, and A. G. W. Leslie, eds. (Warrington, England: SERC Daresbury Laboratory), pp. 80–85.

Otwinowski, Z. (1993). DENZO. In Data Collection and Processing, L. Sawyer, N. Isaacs, and S. Bailey, eds. (Warrington, England: SERC Daresbury Laboratory), pp. 56–62.

Read, R. J. (1986). Improved Fourier coefficients for maps using phases from partial structures with errors. Acta Cryst. *A42*, 140–149.

Reed, R. R. (1981). Transposon-mediated site-specific recombination: a defined in vitro system. Cell *25*, 713–719.

Reed, R. R., and Grindley, N. D. F. (1981). Transposon-mediated site-specific recombination in vitro: DNA cleavage and protein–DNA linkage at the recombination site. Cell *25*, 721–728.

Reed, R. R., and Moser, C. D. (1984). Resolvase-mediated recombination intermediates contain a serine residue covalently linked to DNA. Cold Spring Harbor Symp. Quant. Biol. *49*, 245–249.

Rice, P. A., and Steitz, T. A. (1994a). Refinement of γδ resolvase reveals a strikingly flexible molecule. Structure *2*, 371–384.

Rice, P. A., and Steitz, T. A. (1994b). Model for a DNA-mediated synaptic complex suggested by crystal packing of γδ resolvase subunits. EMBO J. *13*, 1514–1524.

Richards, F. M., and Kundrot, C. E. (1988). Identification of structural motifs from protein coordinate data: secondary structure and first-level supersecondary structure. Prot. Struct. Function Genet. *3*, 71–84.

Rimphanitchayakit, V., and Grindley, N. D. F. (1990). Saturation muta-

genesis of the DNA site bound by the small carboxy-terminal domain of γδ resolvase. EMBO J. *9*, 719–725.

Rimphanitchayakit, V., Hatfull, G. F., and Grindley, N. D. F. (1989). The 43 residue DNA binding domain of γδ resolvase binds adjacent major and minor grooves of DNA. Nucl. Acids Res. *17*, 1035–1050.

Sanderson, M. R., Freemont, P. S., Rice, P. A., Goldman, A., Hatfull, G. F., Grindley, N. D. F., and Steitz, T. A. (1990). The crystal structure of the catalytic domain of the site-specific recombination enzyme γδ resolvase at 2.7 Å resolution. Cell *63*, 1323–1329.

Schultz, S. C., Shields, G. C., and Steitz, T. A. (1990). Crystallization of *Escherichia coli* catabolite gene activator protein with its DNA binding site. The use of modular DNA. J. Mol. Biol. *213*, 159–166.

Schumacher, M. A., Choi, K. Y., Zalkin, H., and Brennan, R. G. (1994). Crystal structure of LacI member, PurR, bound to DNA: minor groove binding by alpha helices. Science *266*, 763–770.

Sluka, J. P., Horvath, S. J., Glasgow, A. C., Simon, M. I., and Dervan, P. D. (1990). Importance of minor groove contacts for recognition of DNA by the binding domain of Hin recombinase. Biochemistry *29*, 6551–6561.

Stark, W. M., Grindley, N. D. F., Hatfull, G. F., and Boocock, M. R. (1991). Resolvase-catalysed reactions between *res* sites differing in the central dinucleotide of subsite I. EMBO J. *10*, 3541–3548.

Stark, W. M., and Boocock, M. R. (1994). The linkage change of a knotting reaction catalysed by Tn3 resolvase. J. Mol. Biol. *239*, 25–36.

Wang, B. C. (1985). Resolution of phase ambiguity in macromolecular crystallography. Meth. Enzymol. *115*, 90–112.

Weiss, M. A., Ellenberger, T. E., Wobbe, C. R., Lee, J. P., Harrison, S. C., and Struhl, K. (1990). Folding transition in the DNA-binding domain of GCN4 on specific binding to DNA. Nature *347*, 575–578.